

Published in final edited form as:

J Pediatr Surg. 2010 January ; 45(1): 52–58. doi:10.1016/j.jpedsurg.2009.10.010.

Surgical implantation of a bioengineered internal anal sphincter[★]

Mohamed Hashish^a, Shreya Raghavan^b, Sita Somara^b, Robert R. Gilmont^b, Eiichi Miyasaka^a, Khalil N. Bitar^b, and Daniel H. Teitelbaum^{a,*}

^aSection of Pediatric Surgery, University of Michigan, Mott Children's Hospital F3970, Box 0245, Ann Arbor, MI 48109-0245, USA

^bGI Molecular Motors Lab, Department of Pediatrics, Gastroenterology, University of Michigan, Ann Arbor, MI 48109-0245, USA

Abstract

Purpose—Fecal incontinence is a common disorder that can have devastating social and psychological consequences. However, there are no long-term ideal solutions for such patients. Although loss of continence is multifactorial, the integrity of the internal anal sphincter (IAS) has particular significance. We previously described the development of 3-dimensional bioengineered constructs using isolated smooth muscle tissue from donor C57BL/6 IAS. We hypothesized that the bioengineered ring constructs would retain cellular viability and promote neovascularization upon implantation into a recipient mouse.

Methods—Internal anal sphincter ring constructs were surgically implanted into the subcutaneous tissue of syngeneic C57BL/6 mice and treated with either fibroblastic growth factor 2 (0.26 µg daily) or saline controls using a microosmotic pump. Internal anal sphincter constructs were harvested after 25 days (range, 23–26 days) and assessed morphologically and for tissue viability.

Result—Gross morphology showed that there was no rejection. Rings showed muscle attachment to the back of the mouse with no sign of inflammation. Fibroblastic growth factor 2 infusion resulted in a significantly improved histologic score and muscle viability compared with the control group.

Conclusions—Three-dimensional bioengineered IAS rings can be successfully implanted into the subcutaneous tissue of recipient mice. The addition of fibroblastic growth factor 2 led to improved muscle viability, vascularity, and survival. This approach may become a feasible option for patients with fecal incontinence.

Keywords

Internal anal sphincter; Fibroblastic growth factor 2; Incontinence; Tissue engineering

Fecal incontinence is the involuntary loss of solid or liquid stool or flatus. Epidemiologic studies have shown that fecal incontinence affects 2% to 15% of the population including people of all ages from childhood to the elderly, thus making it a common disorder, which

[★]This work was supported by National Institutes of Health grant 2R01DK042876 and 5R01DK071614 (to K. Bitar) and a Research Advisor Committee Grant by the Department of Surgery, University of Michigan (to D.H. Teitelbaum). The work was also supported with the help of the National Cancer Institute through the University of Michigan's Cancer Center Support Grant (5 P03 CA46592).

© 2010 Elsevier Inc. All rights reserved.

*Corresponding author. Tel.: +1 734 936 8464; fax: +1 734 936 9784. dttlbm@umich.edu (D.H. Teitelbaum).

Presented at the 40th Annual Meeting of the American Pediatric Surgical Association, Fajardo, Puerto Rico, May 28–June 1, 2009.

can lead to a dramatically negative impact on their quality of life [1,2]. Although the control of continence is multifactorial, the integrity of the internal anal sphincter (IAS) has particular significance to continence. The neuromuscular mechanisms that control the IAS are poorly understood; however, the IAS is characterized by the ability to maintain basal tone, as well as to relax, allowing for the passage of feces [3,4]. The loss of IAS function because of congenital anomalies, or trauma, or aging is a critical factor contributing to fecal incontinence. Unfortunately, there are no long-term successful solutions for such patients, either surgically or medically [5,6].

Advances in bioengineering technology have led to the development of a number of organs and tissues. It is now clear that when a 3-dimensional (3-D) structure is kept intact, the physiologic functions of tissues are retained, and the tissue can survive for extended periods of time [7–9]. Challenges, however, remain in gaining adequate long-term viability after implantation into a host. We have previously developed a 3-D bioengineered IAS in which harvested IAS from a donor self-organize inside a loose fibrin gel. The resulting tissues are stable for more than 6 weeks in culture without deterioration of function. We have successfully bioengineered 3-D physiologic models of IAS in vitro using isolated sphincter smooth muscle cells (SMCs) from rabbit, mice, and human IAS. These bioengineered IAS rings exhibited physiologic behavior that is functionally similar to smooth muscle in vivo [10–12]. The long-term goal of tissue engineering is to maintain long-term viability of engineered tissue and to eventually implant the IAS into a recipient. However, a major limitation is the lack of a vasculature within the tissue construct. This lack of a vasculature limits oxygen diffusion to the cells resulting in the loss of viability. It therefore becomes essential to promote neovascularization within the bioengineered tissue [13]. There have been several studies where tissue constructs have been engineered in vitro and then implanted into recipient animals. However, the degree of success varies according to the ability of the construct to promote the generation of new blood vessels [14–17]. Many recent approaches have suggested improved neovascularization with the use of recombinant angiogenic growth factors including vascular endothelial growth factor or basic fibroblast growth factor (FGF) [18–23]. In this study, we describe the subcutaneous implantation model of bioengineered IAS constructs along with the constant infusion of FGF-2. We further hypothesized that these constructs would retain cellular viability and promote neovascularization upon surgical implantation into syngeneic mice, and that this would be enhanced with the use of FGF-2.

1. Materials and methods

1.1. Bioengineered IAS constructs

The development of 3-D bioengineered IAS constructs has been previously described. Briefly, isolated SMCs are grown in a fibrin gel casting in an in vitro setting [14–16]. In the present study, we developed 3-D bioengineered IAS from isolated mouse IAS SMCs. Briefly, the IAS, consisting of the distal most 3 mm of the circular muscle layer, ending at the junction of skin and mucosa, and the distal colon were removed by sharp microdissection. The tissues were rapidly cleaned and stripped of a connective tissue in ice-cold carbonated Krebs solution containing 2% penicillin-streptomycin. Using sterile technique, isolated mouse IAS cells were seeded onto a fibrin mold (Slygard, Dow Corning, Midland, MI; polydimethylsiloxane), which allows cells to self-align and form a ring within a 5- to 10-day period of time.

1.2. IAS implantation and harvesting

1.2.1. Animals—C57BL/6J female, specific pathogen-free mice (8 week old; Jackson Laboratory, Bar Harbor, ME) were maintained under temperature-, humidity-, and light-

controlled conditions. The studies conform to the Guidelines for the Care and Use of Laboratory Animals established by the University Committee on Use and Care of Animals at the University of Michigan, and protocols approved by that committee (No. 09714).

1.2.2. Surgical procedure—Sterile pumps containing recombinant FGF-2 (see below) dissolved in sterile phosphate-buffered saline (PBS) were prepared. Anesthetized mice had the surgical area in the back of the mice shaved and prepared with surgical scrub and alcohol. A 2-cm skin incision was made in the upper part of the back of the mice (midscapular incision). Care was taken to cut only the skin and not the underlying tissues. A subcutaneous pocket was created, which was large enough to fit the microosmotic pump. The pump (Alzet microosmotic pump, model 1004; Durect Corporation, Cupertino, CA) and the attached sterile polyethylene catheter (ID 0.76 mm) were kept in sterile 0.9% saline at 37°C for at least 48 hours before implantation to ensure for equilibrium and precise delivery of growth factor at a delivery rate of 0.11 $\mu\text{L}/\text{h}$, and total volume was 100 μL (Fig. 1). Recombinant FGF-2 (ProSpec-Tany TechnoGene Ltd, Israel) was prepared by dissolving 10 μg of FGF-2 in 100 μL of PBS, allowing for the delivery of 0.26 $\mu\text{g}/\text{day}/\text{mouse}$. In controls only PBS was given.

After the pump and the attached catheter were inserted into the subcutaneous pocket, the IAS ring was inserted into the same pocket approximately 0.5 cm away. One small nonabsorbable suture (6-0 polypropylene) was placed loosely around the implanted construct to mark its position. After the implanted ring was secured in place, we directed the tip of the polyethylene catheter toward the implanted construct and fixed it to the underlying muscle to prevent excess movement and to direct the delivered substance toward the implanted IAS. The skin incision was then closed with 4-0 polyglycolic acid sutures. The animals were returned to cages for recovery in standard fashion for approximately 25 days. A total of 10 ring constructs were implanted in this manner (5 mice received FGF-2, and 5 control mice).

1.2.3. Construct harvest—Mice were sacrificed between 23 and 26 days postimplantation (mean, 25 days) using carbon dioxide asphyxiation. The previous incision was reentered and the construct removed from the surrounding tissue after localization of the polypropylene suture site. The implanted IAS construct was then harvested for morphologic assessment.

1.3. Gross and histologic morphology

The gross appearance of the implanted ring construct was evaluated by visual and tactile examination upon harvest. Parameters assessed included color, size, and texture. The IAS constructs were immediately divided into 2 halves, and sections were immediately fixed in 10% buffered formalin. Formaldehyde fixed tissues were dehydrated, embedded in paraffin, and sectioned transversely (5- μm thickness) and were stained with H&E for morphologic analysis.

1.3.1. Histologic scoring system—Examination was performed using standard setting of a Nikon TS 100 microscope (Nikon Corp., Tokyo, Japan). Histologic assessment of tissue viability was made according to a viability scoring system, as previously described, and modified slightly by our laboratory [24,25]. The histologic assessment score (Table 1) ranged from 0 to 5 and was based on 3 criteria: morphology of the muscle, presence or absence of degeneration of the muscle fibers, and amount of blood vessel in-growth. Additional analysis was performed to better quantify the mean number of blood vessels seen in 5 distinct high-powered fields (HPFs), with the maximal number of nonoverlapping vessels being scored. Furthermore, the number of muscle fibers was counted and represents

the number of muscle fibers in one HPF. Finally, the mean muscle fiber size was also recorded for each IAS. For each examined IAS ring, the value measured was based on the mean score in a minimum of 5 fields at 200× total magnification, and the final score was computed by adding the score for each half, the result represented an n = 1 result.

1.4. Statistical analysis

Data are reported as mean ± SD. Results were analyzed using *t* tests for comparison of 2 means using Prism software (GraphPad Software, Inc, San Diego, CA). A value of *P* < .05 was considered to be statistically significant.

2. Results

2.1. Gross macroscopic morphology

Mice showed no gross abnormalities upon the harvest of the construct (Fig. 1). All mice maintained normal weight gain and activity postimplantation and showed no evidence of wound infection; survival was 100%. The overall gross appearance of the implanted IAS is summarized in Table 2. All rings showed muscle attachment to the back of the mouse, with no discoloration or signs of inflammation. Interestingly, superficial capillaries were visible in multiple sites on the FGF-2–treated rings during harvesting, indicating a gross suggestion of healthy vascularization. Upon harvest, IAS rings showed good bleeding in 4 of the FGF-2–treated mice, whereas 1 graft was darker with a reduced amount of bleeding compared with the others. There was no significant difference in the ring size before and after implantation in 4 of the 5 FGF-2 mice. Size variability, however, was much greater among the mice in the control group (Table 2). Texture of the harvested ring was soft in 4 of the FGF-2 mice, whereas the rings in 2 of the control group had a firm texture.

2.2. Histologic scoring

The overall histologic results are summarized in Table 3 and Fig. 2. There was a highly significant difference (*P* < .001; Table 3) between the control group (3.4 ± 1.8 ; range, 3–7) and the FGF-2 group (8.0 ± 1.6 ; range, 6–10) for the total histologic score, strongly supporting a greater degree of viability of the postimplanted IAS construct treated with FGF-2. Several differences were seen with regard to individual components of the grading system. There was a significant difference between the 2 groups regarding the morphologic score (FGF-2 group $3.0 \pm .7$ versus control group 1.2 ± 0.8 ; *P* < .05). Degree of vascularity showed multiple large-sized vessels in 4 of the 5 FGF-2 treated rings (1.6 ± 0.54), whereas only 2 IAS rings in the control group had blood vessels that could be clearly identified (0.2 ± 0.4). Although qualitatively there was no statistically significant difference in the blood vessel score, the mean number of blood vessels was seen to be significantly increased (*P* < .01) in the FGF-2–treated group (Table 3). There was no significant difference between study groups regarding the degree of muscle degeneration (*P* > .05). However, there was a significant increase in the overall number of muscle fibers and size of the muscle fibers in the FGF-2–treated group (Table 3; *P* < .05).

3. Discussion

Despite the high incidence of the fecal incontinence, there are no long-term successful solutions for such patients. Although the integrity of the IAS plays a critical role in maintaining anal continence, little is known about the mechanisms underlying the IAS function and physiology. We have successfully developed 3-D bioengineered IAS rings from IAS SMCs of donor mice. To our knowledge, this is the first published report that confirmed that an IAS construct can be successfully implanted subcutaneously into a mouse and remain viable for 3 weeks. Clearly, one of the greatest challenge is keeping the construct

viable during implantation, with generation of new blood vessels that would promote the long-term survival of the IAS construct [13,26]. There have been several research studies describing the methods of surgical implantation of a bioengineered construct into the recipient mice. Although the target site of implantation has varied considerably between studies, the most common sites were subcutaneously [14,19,27], Intraperitoneally around the omentum or in the orthotopic location of the original tissue (ie, the myocardium for cardiac tissue implant) [28–30]. In all sites, the successful implantation depended on neovascularization. In our study, we described subcutaneous implantation in the upper part in the back of the mice. We preferred this area for implantation because this area was felt to be safe and far from being injured by the mouse. In addition, this location has been found to have sufficient space for placement of the pump and IAS.

One of the most important limitations of successful surgical implantation of a tissue construct is the poor in-growth of new blood vessels, which results in cell loss owing to hypoxic cell death during the early postimplantation stage [31]. Many attempts have been made to overcome this problem and stimulate vasularization by using recombinant angiogenic growth factors including vascular endothelial growth factor or basic FGF. The use of constant infusion of FGF-2 over 14 days with a microosmotic pump increased tumour vascularity, blood flow, and even the chemotherapy uptake [20]. Also, FGF-2 increased vascularization and improves the process of wound healing in ischemic tissue [21]. Recently, Marra et al proved that delivery of FGF-2 for 14-days in vivo resulted in cell survival and enhanced vascularization of adipose tissue, which decreased the time required for successful vascularization and accelerated the treatment process [32].

In our study, we described sustained local infusion of recombinant human FGF-2 using a microosmotic pump. The use of such pumps provided constant infusion over the postimplantation period without observed evidence of systemic effects and allowed increased efficiency of the drug owing to its proximity [33]. Dosing of FGF-2 varies among researches between a dose of 0.1 to 0.5 $\mu\text{g}/\text{d}$ [34]. Dosing depends on the duration of delivery and the optimal goal. In our study, we delivered an average dose approximately 0.26 $\mu\text{g}/\text{d}$ with a maximum dose of 7 μg over the entire time of implantation. This dose was found to be quite suitable for graft viability and for the promotion of vascularization.

Many authors have described implantation of tissue constructs in vivo, but the results of implantation have been variable [35,36]. In our study, no signs of rejection were found in the implanted rings because of the use of syngeneic tissue. All rings showed good muscle attachment to the recipient mouse, without signs of inflammation. Interestingly, blood vessels were visible on many of the FGF-2-treated rings, indicative of healthy vascularization. Our histologic results showed that there was a highly significant difference between the control and FGF-2 group, which also demonstrated the high viability of the postimplanted IAS construct treated with growth factor. Although there are few previous comparative studies regarding histologic scores of implanted constructs, our result matched previous investigators who showed the importance of FGF-2 in maintaining viability and neovascularization of implanted tissue [32].

Our laboratories have recently reported the successful development of human IAS, which also opens up the possibility of translating this application to clinical usage [37].

We conclude that 3-D bioengineered rings can be successfully implanted in subcutaneous tissue. The addition of FGF-2 may well lead to improved tissue viability, cellular integrity, and improved vascularization. This approach may become a viable future option for patients with fecal incontinence.

References

1. Nelson R, Norton N, Cautley E, et al. Community-based prevalence of anal incontinence. *JAMA* 1995;274:559–561. [PubMed: 7629985]
2. Perry S, Shaw C, McGrother C, et al. Prevalence of faecal incontinence in adults aged 40 years or more living in the community. *Gut* 2002;50:480–484. [PubMed: 11889066]
3. Sultan AH, Kamm MA, Hudson CN, et al. Third degree obstetric anal sphincter tears: risk factors and outcome of primary repair. *BMJ* 1994;308:887–891. [PubMed: 8173367]
4. Jones OM, Brading A, Mortensen N. The physiology, pharmacology and therapeutic manipulation of the internal anal sphincter. *Can J Gastroenterol* 2002;16:249–257.
5. da Silva G, Jorge J, Belin B, et al. New surgical options for fecal incontinence in patients with imperforate anus. *Dis Colon Rectum* 2004;47:204–209. [PubMed: 15043291]
6. Whitehead W, Wald A, Norton N. Treatment options for fecal incontinence. *Dis Colon Rectum* 2001;44:131–142. [PubMed: 11805574]
7. Dennis R, Kosink IP. Excitability and isometric contractile properties of mammalian skeletal muscle constructs engineered in vitro. *In Vitro Cell Dev Biol Anim* 2000;36:327–335. [PubMed: 10937836]
8. Dennis RG, Kosnik PE, Gilbert ME, et al. Excitability and contractility of skeletal muscle engineered from primary cultures and cell line. *Am J Physiol Cell Physiol* 2001;280:288–295.
9. Dennis, R.; Kosink, IP. Mesenchymal cell culture: instrumentation and methods for evaluating engineered muscle. In: Atala, A.; Lanza, R., editors. *Methods in tissue engineering*. San Diego (Calif): Academic; 2002. p. 9
10. Hecker L, Baar K, Dennis R, et al. Development of a three-dimensional physiological model of the internal anal sphincter bioengineered in vitro from isolated smooth muscle cells. *Am J Physiol Gastrointest Liver Physiol* 2005;289:188–196.
11. Bitar K, Makhlof G. Relaxation of isolated gastric smooth muscle cells by vasoactive intestinal peptide. *Science* 1982;216:513–533.
12. Bitar KN, Makhlof GM. Specific opiate receptors on isolated mammalian gastric smooth muscle cells. *Nature* 1982;297:72–74. [PubMed: 6122163]
13. Birla RK, Borschel GH, Dennis RG. In vivo conditioning of tissue-engineered heart muscle improves contractile performance. *Artificial Organs* 2005;29:866–875. [PubMed: 16266299]
14. Shimizu T, Yamato M, Isoi Y, et al. Fabrication of pulsatile cardiac tissue grafts using a novel 3-dimensional cell sheet manipulation technique and temperature-responsive cell culture surfaces. *Circ Res* 2002;90:e40. [PubMed: 11861428]
15. Eschenhagen T, Didie M, Munzel F, et al. 3D engineered heart tissue for replacement therapy. *Basic Res Cardiol* 2002;97:1146–1152. [PubMed: 12479248]
16. Selden R, Skoskiewicz M, Howie K, et al. Implantation of genetically engineered fibroblasts into mice: implications for gene therapy. *Science* 1987;236:714–718. [PubMed: 3472348]
17. Nisolle M, Casanas-Roux F, Marbaix E, et al. Transplantation of cultured explants of human endometrium into nude mice. *Hum Reprod* 2000;15:572–577. [PubMed: 10686198]
18. Mazue G, Bertolero F, Jacob C, et al. Preclinical and clinical studies with recombinant human basic fibroblast growth factor. *Ann N Y Acad Sci* 1991;638:3329–3340.
19. Steffens L, Wenger A, Stark GB, et al. In vivo engineering of a human vasculature for bone tissue engineering applications. *J Cell Mol Med*. 2009 [Epub ahead of print].
20. Davies M, Burke D, Carnochan P, et al. Basic fibroblast growth factor infusion increases tumour vascularity, blood flow and chemotherapy uptake. *Acta Oncol* 2002;41:84–90. [PubMed: 11990524]
21. Uhl E, Barker JH, Bondar I, et al. Basic fibroblast growth factor accelerates wound healing in chronically ischaemic tissue. *Br J Surg* 1993;80:977–980. [PubMed: 8402094]
22. Lindner V, Majack RA, Reidy MA. Basic fibroblast growth factor stimulates endothelial regrowth and proliferation in denuded arteries. *J Clin Invest* 1990;85:2004–2008. [PubMed: 2347923]
23. Roberts-Clark DJ, Smith AJ. Angiogenic growth factors in human dentine matrix. *Arch Oral Biol* 2000;45:1013–1016. [PubMed: 11000388]

24. Tang ATM, Hasleton PS, Heid H, et al. Quantification of early damage in latissimus dorsi muscle grafts. *Muscle Nerve* 1998;21:1451–1456. [PubMed: 9771669]
25. Kwan M, Tam E, Lo S, et al. The time effect of pressure on tissue viability: investigation using an experimental rat model. *Exp Biol Med* 2002;232:481–487.
26. Bursac N, Papadaki M, Cohen RJ, et al. Cardiac muscle tissue engineering: toward an in vitro model for electrophysiological studies. *Am J Physiol Cell Physiol* 1999;277:H433–H444.
27. Baek CH, Ko YJ. Characteristics of tissue-engineered cartilage on macroporous biodegradable PLGA scaffold. *Laryngoscope* 2006;116:1829–1834. [PubMed: 17016212]
28. Sakai T, Li RK, Weisel RD, et al. The fate of a tissue-engineered cardiac graft in the right ventricular outflow tract of the rat. *J Thorac Cardiovasc Surg* 2001;121:932–942. [PubMed: 11326237]
29. Leor J, Aboulafia-Etzion S, Dar A, et al. Bioengineered cardiac grafts: a new approach to repair the infarcted myocardium? *Circulation* 2000;102:III56–III61. [PubMed: 11082363]
30. El-Akouri RR, Molne J, Groth K, et al. Rejection patterns in allogeneic uterus transplantation in the mouse. *Hum Reprod* 2006;21:436–442. [PubMed: 16253976]
31. Griffith CK, Miller C, Sainson RC, et al. Diffusion limits of an in vitro thick prevascularized tissue. *Tissue Eng* 2005;11:257–266. [PubMed: 15738680]
32. Marra KG, Defail AJ, Clavijo-Alvarez JA, et al. FGF-2 enhances vascularization for adipose tissue engineering. *Plast Reconstr Surg* 2008;121:1153–1164. [PubMed: 18349632]
33. Urquhart J, Fara JW, Willis KL. Rate-controlled delivery systems in drug and hormone research. *Annu Rev Pharmacol Toxicol* 1984;24:199–236. [PubMed: 6375546]
34. Scholz D, Ziegelhoeffer T, Helisch A, et al. Contribution of arteriogenesis and angiogenesis to postocclusive hindlimb perfusion in mice. *J Mol Cell Cardiol* 2002;34:775–787. [PubMed: 12099717]
35. Xia Z, Taylor PR, Locklin RM, et al. Innate immune response to human bone marrow fibroblastic cell implantation in CB17 scid/beige mice. *J Cell Biochem* 2006;98:966–980. [PubMed: 16795075]
36. Samsudin OC, Aminuddin BS, Munirah S, et al. In vitro development of autologous tissue engineered human articular neocartilage for orthopaedic surgery. *Med J Malaysia* 2004;59 Suppl B:15–16. [PubMed: 15468796]
37. Somara S, Gilmont RR, Dennis RG, Bitar KN. Bioengineered internal anal sphincter derived from isolated human internal anal sphincter smooth muscle cells. *Gastroenterology* 2009;137(1):53–61. [PubMed: 19328796]

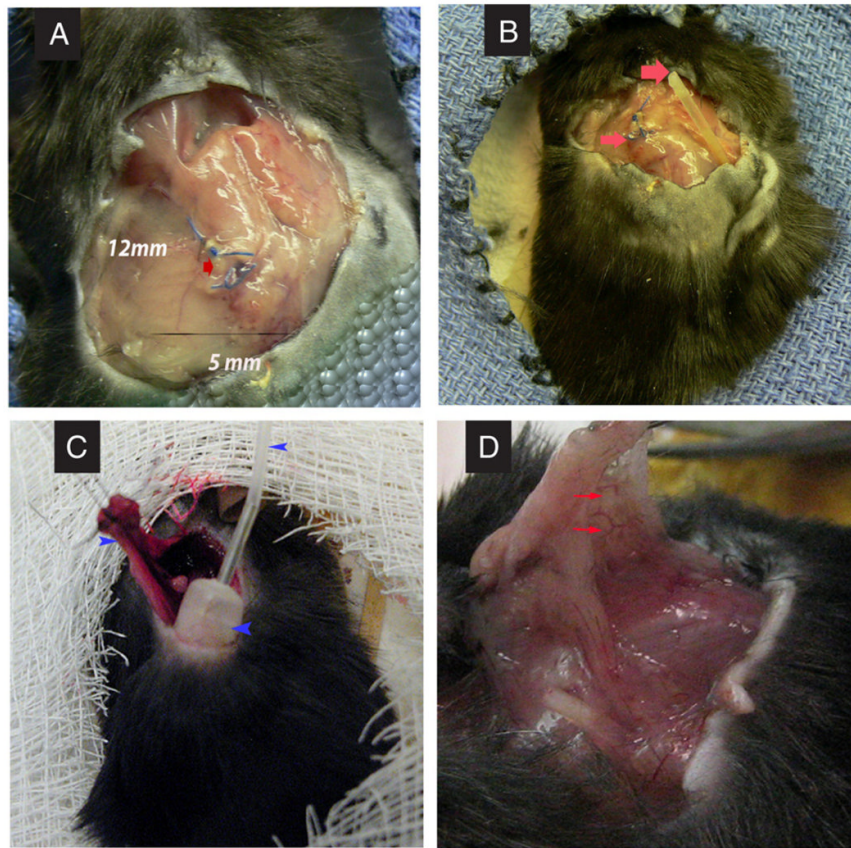


Fig. 1. Operative photographs. A, The arrow shows the implanted IAS ring with nonabsorbable suture around it. Dimensions of graft are marked: 12 and 5 mm. B, Implanted IAS ring (small arrow) and tip of microosmotic pump catheter near the IAS graft (large arrow). C, One arrow shows the implanted IAS ring at time of harvest with the other 2 arrows (pointing to the left) show the pump with the attached catheter. D, Implanted IAS ring at time of harvest with arrows showing multiple visible blood vessels adjacent to the graft.

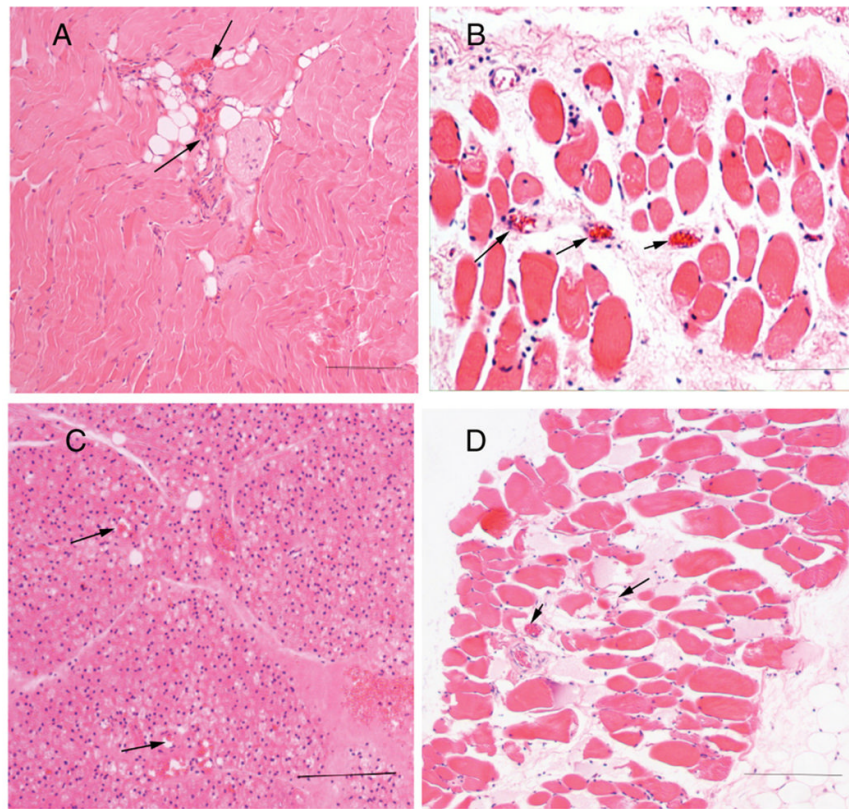


Fig. 2. Histomicrographic appearance of IAS implants. Bar represents 200 μm . A and B, Implanted IAS ring from FGF-2 group. A, Note the tightly distributed muscle fiber bundles. Note the well-formed peripheral nuclei in each cell and central blood vessels between muscle bundles (arrows). B, Cross section of IAS. Note the well-formed muscle fibers with peripheral nuclei and numerous blood vessels (arrows) in between bundles. C and D, Implanted IAS ring from control group. C, Note the distortion of the muscle fibers with few vessels and numerous nuclei consistent with loss of muscle cell size. D, Cross section of IAS. Note the loss of muscle fibers and increased fat cells in between cells. Note also a reduction in the number of blood vessels (arrows).

Table 1

Histologic scoring devised to assess the viability of the implanted IAS construct

| Criteria | Score |
|--|-------|
| 1. Morphology of the muscle | |
| - Packed polygonal muscle fiber profiles with normal shape | 2 |
| - Mild separation of muscle fiber with preserve of shape | 1 |
| - Marked separation of the muscle fiber with distortion of the shape | 0 |
| 2. Degeneration of fiber | |
| - No degeneration | |
| Little variation in muscle fiber size or shape. | 2 |
| Cytoplasm is uniform, and small, peripherally located nuclei are abundant. | |
| - Mild degeneration | |
| Numerous nuclei with round contours are present, muscle fibers are replaced by fibro-fatty tissue, and abnormal variation in fiber size is due to atrophy of some and the hypertrophy of others. | 1 |
| - Marked degeneration | |
| Muscle fibers become necrotic and destruction of muscle fibers with the replacement of the muscle by fibrous tissue. | 0 |
| 3. Blood vessels | |
| - Present and easily seen | 1 |
| - Absent or difficult to see | 0 |

Table 2

Gross appearance of IAS postharvesting

| Criteria | FGF-2 (n = 5) | Control (n = 5) |
|-------------------|---------------|-----------------|
| Color: | | |
| Red | 4 | 2 |
| Darker or whitish | 1 | 2 |
| Black | 0 | 1 |
| Size: | | |
| Same or near | 4 | 2 |
| Increase | 1 | 1 |
| Decrease | 0 | 2 |
| Texture: | | |
| Soft | 4 | 2 |
| Firm | 1 | 3 |

Table 3

Histologic scoring of the 2 study groups

| Group | Morphology score (0-4) | Muscle fiber degeneration (0-4) | Blood vessel in-growth (0-2) | Mean number of blood vessels per HPF | Mean number of muscle fibers per HPF | Mean fiber diameter (μm) | Total score (0-10) |
|---------|------------------------|---------------------------------|------------------------------|--------------------------------------|--------------------------------------|---------------------------------------|--------------------|
| FGF-2 | 3.0 \pm 0.7** | 3.4 \pm 0.6 | 1.6 \pm 0.5 | 5.6 \pm 2.0* | 5.0 \pm 0.3** | 32.0 \pm 5.7** | 8.0 \pm 1.6* |
| Control | 1.2 \pm 0.8 | 2.0 \pm 0.7 | 0.2 \pm 0.4 | 1.2 \pm 0.4 | 2.6 \pm 0.5 | 20.0 \pm 5.0 | 3.4 \pm 1.8 |

Result was given as the mean \pm SD.* $P < .01$.** $P < .05$ using paired t test.